

AD-A123 313

TEMPORAL IMAGE NORMALIZATION(U) DEFENSE MAPPING AGENCY
HYDROGRAPHIC/ TOPOGRAPHIC CENTER WASHINGTON DC
D J GERSON ET AL. 04 JAN 83

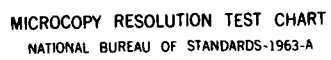
1/1

UNCLASSIFIED

F/G 9/2

NL





REPORT DOCUMENTATION PAGE		READ INSTRUCTIONS BEFORE COMPLETING FORM
1. REPORT NUMBER None	2. GOVT ACCESSION NO. AD-A123313	3. RECIPIENT'S CATALOG NUMBER
4. TITLE (and Subtitle) TEMPORAL IMAGE NORMALIZATION		5. TYPE OF REPORT & PERIOD COVERED Final Report
		6. PERFORMING ORG. REPORT NUMBER
7. AUTHOR(s) Donald J. Gerson, Lynn K. Fehrenbach, Dennis McTernan		8. CONTRACT OR GRANT NUMBER(s)
9. PERFORMING ORGANIZATION NAME AND ADDRESS DMA Hydrographic/Topographic Center 6500 Brooks Lane Washington, D.C. 20315		10. PROGRAM ELEMENT, PROJECT, TASK AREA & WORK UNIT NUMBERS
11. CONTROLLING OFFICE NAME AND ADDRESS N/A		12. REPORT DATE March 1983
		13. NUMBER OF PAGES 10
14. MONITORING AGENCY NAME & ADDRESS (if different from Controlling Office) N/A		15. SECURITY CLASS. (of this report) UNCLASSIFIED
		15a. DECLASSIFICATION/DOWNGRADING SCHEDULE
16. DISTRIBUTION STATEMENT (of this Report) Unlimited		
17. DISTRIBUTION STATEMENT (of the abstract entered in Block 20, if different from Report) Unlimited		
18. SUPPLEMENTARY NOTES Presented at 1983 ACSM-ASP Convention March 13-18, 1983, Washington, D.C.		
19. KEY WORDS (Continue on reverse side if necessary and identify by block number) Image Processing, Digital Imagery, Remote Sensing		
20. ABSTRACT (Continue on reverse side if necessary and identify by block number) Temporal Image Normalization (TIN) is defined as a process which removes most effects of sun angle, look angle, and atmosphere from temporally separated images of the same area. This process is usually used to prepare images for further analysis. Three approaches are used in the TIN are: (1) analysis of image and scene content (techniques come from the fields of photographic science and photometry), (2) analysis of atmospheric and ephermeris data (techniques come		

DTIC
ELECTE

JAN 12 1983

E

DD FORM 1473

1 JAN 73

EDITION OF 1 NOV 65 IS OBSOLETE

UNCLASSIFIED

SECURITY CLASSIFICATION OF THIS PAGE (When Data Entered)

83 61 12 614

AD A123313

DTIC FILE COPY

20. (Cont'd)

from meteorological theory and usually require extensive measurements of the atmosphere), and (3) combinations of approaches 1 and 2. Five TIN algorithms are discussed and three of them are evaluated in this paper according to the quality of their output images and the degree of normalization achieved.

A high degree of normalization was obtained with excellent information preservation in black and white aerial photos of terrestrial scenes. The results for color imagery of shallow, clear water areas were far less successful, although some degree of normalization was achieved. The algorithm used on Landsat imagery showed limited success in normalizing only the Band 5 data.

TEMPORAL IMAGE NORMALIZATION

To be Presented at the
1983 ACSM-ASP Convention
March 13-18, 1983
Washington, D.C.

Accession For	
NTIS GRA&I	<input checked="checked" type="checkbox"/>
DTIC TAB	<input type="checkbox"/>
Unannounced	<input type="checkbox"/>
Justification	
By _____	
Distribution/	
Availability Codes	
Dist	Avail and/or Special
A	



D. Gerson

L. Fehrenbach

CLEARED BY OASD(PA) 4 Jan 1983

OASD #0026

TEMPORAL IMAGE NORMALIZATION
D. J. Gerson, and L. K. Fehrenbach
Defense Mapping Agency Hydrographic/Topographic Center
Washington, D.C. 20315

ABSTRACT

Temporal Image Normalization (TIN) is defined as a process which removes most effects of sun angle, look angle, and atmosphere from temporally separated images of the same area. This process is usually used to prepare images for further analysis. Three are used in TIN are: (1) analysis of image and scene content (techniques come from the fields of photographic science and photometry), (2) analysis of atmospheric and ephemeris data (techniques come from meteorological theory and usually require extensive measurements of the atmosphere), and (3) combinations of approaches 1 and 2. Five TIN algorithms are discussed, and three of them are evaluated in this paper according to the quality of their output images and the degree of normalization achieved. A high degree of normalization was obtained with excellent information preservation in black and white aerial photos of terrestrial scenes. The results for color imagery of shallow, clear water areas were far less successful, although some degree of normalization was achieved. The algorithm used on Landsat imagery showed limited success in normalizing only Band 5 data.

INTRODUCTION

In general, it may be said that temporal image normalization refers to the removal of time-varying anomalies from an image, regardless of their origin. The ideal definition is not achievable at this time due to limits within state-of-the-art technology. An attainable definition, however, is as follows:

A process which, if applied to two temporally separated images, removes most of the effects of sun angle, look angle, and atmosphere from each image, thus causing them to look "similar" with minimal sacrifice in "information" content.

This definition deals with the observational aspects of TIN, and eliminates those aspects which cannot be managed at the present time, such as variations in snow cover and crop maturation. Normalization for hydrographic applications varies somewhat from the approach used for topographic applications. In imagery of shallow, clear water areas, electromagnetic energy is sensed through a column of air and water with a discontinuity at the interface. This is a far more complex media than the atmospheric column which is involved in the collection of topographic imagery. Specific temporal effects which perturb hydrographic imagery are tidal water depth variations, bottom material changes, and changes in water surface characteristics, which cause variations in specular reflectance. These are not addressed by the constrained TIN definition, but are important.

The first of the three approaches used in TIN utilizes only image characteristics such as film density and grey level, and prior knowledge of the reflectance values of ground materials within the scene. This approach compensates for, rather than corrects atmospheric and ephemeris characteristics. The second method utilizes

only measurable data or data of known parameters which affect the physics of the imaging process, such as atmospheric characteristics and ephemeris data. These data are used to develop corrections which are applied to an image. The imaging process obviously must also be known and controlled, but no measurements are taken from the resultant image. This technique utilizes both atmospheric and radiative transfer models. The third approach uses both image-related and data-related measurements.

Five algorithms are discussed in detail in this paper; of these the performance of three was evaluated in a series of tests. To assess the degree of temporal normalization possible with each algorithm being tested, a determination of output image quality is needed so that information loss can be measured. It is also necessary to measure similarity between the output images. Metric and subjective evaluation techniques were utilized for these purposes in the experiment to be described.

The metric evaluation techniques that were attempted were: a) an analysis of the power spectrum for normalized images; this was computed using the two dimensional discrete Fourier transform, and b) analysis of the mean and standard deviation of histogram statistics. Another important metric method used in this experiment was the comparison of image content with ground truth. This was particularly important for the evaluation of hydrographic color imagery since the photo-derived data were to be used for obtaining subsurface reflectance measurements.

Statistical analysis of subjectively evaluated image quality was used to quantify the retention of image quality for interpretation purposes. Since each image was rated individually for quality both before and after normalization, the analysis also gave a measure of similarity in image quality.

REVIEW OF STATE-OF-THE-ART (SOTA)

Temporal Image Normalization (TIN) embodies those aspects of applied remote sensing which are capable of developing an image transform that can "normalize" an image according to the definition previously stated. The three approaches to TIN mentioned earlier are derived from distinct scientific disciplines.

Techniques involving the use of image characteristics with some knowledge of image content come from the fields of photographic science and photometry as applied to remote sensing. Techniques involving the use of radiative transfer and atmospheric models, along with ephemeris data, come from meteorological theory. These techniques require extensive measurements of the atmosphere which are beyond those normally available during the imaging process. These measurements, combined with the ephemeris data which usually are available, can be used to compute a normalizing transform which is independent of image content. Other methods applicable to TIN fall into the area of utilizing both the image data and the atmospheric and ephemeris data. Among these methods are multispectral techniques which are applicable to both Landsat and airborne multispectral scanner observations. Other techniques applicable to TIN are available, but were considered outside the scope of this project. These mainly include algorithms which deal with portions of the electromagnetic spectrum outside the visible range.

Analysis of image and scene content

The method utilized in Tests 1 and 2, which will be described later, represents one SOTA technique for analysis of image and scene content. This method is an application (Gerson et al 1981, Piech and Walker 1974, Piech 1980) of a classical reflectance derivation technique (Lillesand 1974). It is based on the use of film density to compute a reflectance value using the minimum scene reflectance and a known reflectance within the scene to derive the relationship between density and reflectance. The reflectance values are then transformed into "pseudodensities" to produce a normalized image.

A closely related technique, (Piech et al 1978, Schimminger 1980) utilizes densities measured from the same material in shadow and sunlit areas on an image. These are plotted on a graph of shadow exposure vs. sun exposure for the same material, and linear regression is used to plot a line. A second line is drawn at a 45° angle to each axis (sun exposure equal to shadow exposure). The point where they intersect is β , the exposure for zero reflectance, since only at this point will sun exposure equal shadow exposure. Next, several values of measured exposure vs. known reflectance are plotted on a graph of exposure vs. reflectance. A regression line is fit to these points, but is forced through the previously determined value of exposure at zero reflectance. This produces α , the exposure vs. reflectance relationship. The α and β derived here are the same as the α and β in Tests 1 and 2. The only difference is in the method of their derivation.

Another related method, (Crouch and Leonard 1979), is fairly similar to both of these and forms the basis for Test 5. In addition it uses regression on several points of known reflectance vs. measured density without using shadow data or minimum reflectance data.

The methods discussed above are applicable to hydrographic imagery to a limited extent. Lyzenga and Polcyn (1979) have attempted to deal with the problems specific to hydrographic imagery with a different approach. Their method entails registering several digital images to one another and then taking the darkest pixel from the group as a reference to compose a new image. This eliminates transient effects such as clouds and specular reflectance. The problem with this method is that other lighting effects cause differences between images in areas unaffected by clouds and specular reflectance. This results in a mottled appearance in the composite image.

Analysis of atmospheric and ephemeris data

Multiple scattering atmospheric radiation models.

Molecules and suspended particulates in the atmosphere scatter and absorb visible and near-visible infrared radiation as it passes through the atmosphere. If the properties of the atmosphere are concentrated enough, radiated energy may be scattered many times as it propagates from source to detector. In order to account for the effects of multiple scattering on imagery, a number of detailed mathematical models and computational procedures of varying complexity have been developed in recent years. An excellent review of these models by Turner (1981) gives several solutions to the radiative transfer equation. These include exact, numerical, and approximate methods.

The exact analytical methods, while highly accurate, are very limited in scope and application. These methods result in solutions to particular problems, frequently eliminating the need for extensive numerical computation. They serve as "standard" solutions against

which approximate methods can be compared. Unfortunately, due to the complex geometries for many multiple scattering problems, an exact analytical solution is not always possible. The numerical methods are also highly accurate, but are tedious to implement. They are mathematical techniques which approximate a solution of the radiative transfer equation. These methods are used in complex situations, where an exact solution is impossible, but approachable through extensive computation. The approximate methods are most adaptable and lowest in cost for most applications. These are elementary methods which use assumptions of atmospheric conditions to reduce computational difficulty, but provide direct solutions. They are limited to specific ranges of validity depending on the method and its assumptions. Some of these models, particularly the numerical and approximate methods, hold great promise for present applications if the necessary data are available for their application.

Atmospheric models using extensive data sets.

Realistic atmospheric modeling that makes use of extensive data sets which have been derived through numerical modeling and verified with small sets of actual observations, has also been used (Dave 1978). Dave describes five models with very specific characteristics intended to simulate atmospheric conditions that have been found to exist in different areas. The models can be used to estimate atmospheric effects on solar radiation of varying wavelength and angle at various heights above the ground. This approach was developed for determining the performance of solar cells and other solar energy devices, but could certainly be adapted for application to TIN purposes.

Atmospheric correction models.

An empirical model for correcting Landsat data as a function of variations in solar zenith angle, haze level, and average reflectance of areas adjacent to the target, but outside the field of view, (Potter 1977) is described in Test 4.

Other modeling techniques.

Additional techniques that could be applied to TIN are available. Those listed seemed to be particularly significant and applicable to present needs.

Combination methods

An algorithm, which uses a combination of image characteristics and atmospheric parameters, is the Tassled Cap algorithm (Kauth et al 1979, Davis and Wilson 1981) and is the subject of Test 3.

APPROACH/DISCUSSION

The most promising and available image normalization algorithms were tested on selected image scenes containing various features of interest for Mapping, Charting, and Geodesy (MC&G). They were evaluated for quality of output image and degree of normalization obtained by the algorithm. Each algorithm was tested against its designated imagery.

The image test set consisted of pairs of temporally separated images which contained the separations (e.g., differing sun angle or look angle), or perturbation (e.g., haze) that the algorithm was intended to normalize. Both images were over the same area, were of approximately the same scale, and contained several characteristics which were relevant to MC&G purposes. In addition, obliquity was negligible, and the images were taken over areas of relatively level terrain. Some of the color hydrographic imagery was not paired since

temporally separated pairs were not always available. The hydrography experiment, however, consisted of normalizing reflectances in the image and comparing them to known reflectances, therefore pairs were not always required.

The image set included monochrome (visible range, B&W), color (visible range), and Landsat (multispectral) pairs, which allowed for the testing of all algorithms. Each roll of film had a 21-step wedge exposed on its leader. These wedges were digitized and became part of the data set. Extensive ground truth was available for all areas. This included maps, surveys of the military bases (Currin and Ingram 1974, Brooke 1974), and an extensive underwater survey of the Bahamas site including bottom reflectance data.

Test 1

This test involves a reflectance calibration technique to normalize black and white terrestrial imagery by removing the effects of variations in sun-angle, look-angle, and haze content between members of sample image pairs. The procedure normalized imagery by using photometric techniques to determine the reflectances of materials within the imagery, then converted these values to densities to derive a normalized image. In addition to the description below, References 2 and 3 give background information on this procedure. This experiment utilized four frames of black and white imagery taken over Ft. Belvoir, Virginia and two frames taken over Ft. Greely, Alaska.

Using the Perkin Elmer Micro-10 microdensitometer at SCIPAR, Inc., the following were scanned: 1) the density wedge, 2) several areas of concrete, preferably not roads or contaminated areas, 3) an area determined to be of minimal reflectance in the image, and 4) the selected 2.5cm x 2.5cm sample areas. A sample size and sample separation of 50 μ m was used.

A SCIPAR algorithm on their VAX 11-780 was then applied to obtain a Density vs. Log Exposure (D-log E) curve for each step wedge scanned. Utilizing the D-log E curve, the minimum reflectance value, and the known reflectance value of concrete, another SCIPAR algorithm was utilized to obtain reflectance values for each pixel in the sample image. The reflectance (R) for each pixel was obtained using:

$$R = \frac{E - \beta}{\alpha} \quad (1)$$

where: E = the exposure of each pixel

α = the inverse slope of the reflectance vs. exposure curve for the scene; determined from the area of known reflectance.

β = the exposure for zero reflectance; determined from the area of maximum density.

The exposure value (E) was determined by using the D-log E curve to convert the density of each pixel obtained in the microdensitometer scan. The value of β is the exposure of the maximum density obtained by using the D-log E curve. The value of α was obtained from:

$$\alpha = \frac{E_k - \beta}{R_k}$$

(2)

where E_k and R_k are the exposure and corresponding reflectance from the area of known reflectance. These relationships are shown in Figure 1.

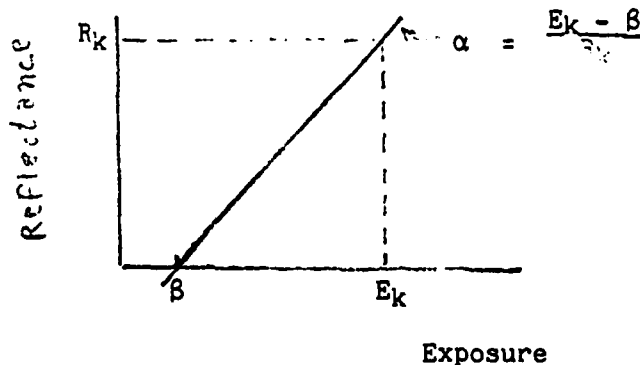


Fig. 1 -
Determination of
Reflectance from
Exposure

These reflectances (R) were then converted to pseudo-densities (D_p) using the following transform function to obtain normalized imagery:

$$D_p = 511.0 - 255.5 \log_{10} R + .5 \quad (3)$$

Test 2

SCIPAR's reflectance calibration technique was next tested for normalizing hydrographic color imagery. Two image pairs plus two additional images were selected from the 1980 DMA Bahamas Photobathymetric Project for digitization. This test proceeded exactly at Test 1 except that sample image pairs were color separated into red, green and blue bands by use of filters, with subsequent application of the SCIPAR technique on each band for normalization (Gerson et al 1981). Color imagery of shallow coastal waters can be used for depth determination, but elimination of variations in surface measured bottom reflectances caused by sun angle, look angle, and atmospheric variations is required to achieve greater accuracy in these measurements. *The calibration was done on a color image of the*

Test 3

The next test was of the Environmental Research Institute of Michigan's (ERIM) Tasseled Cap algorithm for normalizing Landsat imagery by correcting for haze, solar zenith angle, and sensor differences. The key correction is for haze, and was done by the XSTAR algorithm developed by ERIM (and was part of Tasseled Cap.).

This algorithm was designed to operate on Landsat imagery only. The image set consisted of the three "LACIE Segments" (areas approximately 5x6 miles, or 117 scan lines x 196 pixels each) on each of two temporally separated Landsat frames of the Washington, D.C. area. Knowledge of the solar zenith angle was required for this test, as were known corrections for differences between sensing systems. The steps followed in the generation of a normalized image were screening, calculation of a haze diagnostic, correction of the data, and image generation.

Screening.

Initially, known a priori corrections such as correction for solar zenith angle and satellite calibration differences between Landsat 2 and Landsat 3 were made. The data were then transformed into the "Tasseled Cap coordinate system". This system consisted of a plane defined by "Greenness" vs. "Brightness" of the segment, with a third dimension, "Yellowness", perpendicular to the plane, and a fourth

dimension, which primarily contains noise variation, orthogonal to the other three. The data were then screened to eliminate undesired data. that have been developed to reject bad data by a sequence of steps which bound or enclose the Tasseled Cap, cloud, water, and cloud shadow. Pixels outside the enclosure were rejected as bad data. Most bad data points were rejected by this test since the volume enclosed is only a small fraction of the Landsat signal space. Bounds were then established which reject cloud, water, and cloud shadow.

Calculation of a haze diagnostic.

The pixels which are still labeled good after passing the screening tests are used to calculate the diagnostic characteristics. This is done primarily for the purpose of estimating the amount of haze present in the scene. Diagnostic procedures consist of measuring the data average, the soil mean, and green arm mean (Kauth 1979).

Correction of the data.

The output of the diagnostics is used to calculate the haze correction. Both the solar zenith angle correction and the haze correction are then applied in one step to the original raw data in order to avoid developing round-off errors.

Image generation.

Corrected data can then be used to make normalized images. The only additional requirement was to analyze the entire set of scenes to be produced to determine the brightest level desired. This was to insure that the image was within the dynamic range of the film. The exposure for that brightest level in all color separation negatives was then determined and the derived values were used for generation of all scenes to be normalized.

Test 4

The Lockheed Electronics Company, Inc. ATCOR algorithm (Potter 1977) normalizes Landsat imagery by correcting the multispectral scanner (MSS) response as a function of variations in solar zenith angle, haze level, and average reflectance of areas adjacent to the target, but outside the field of view. This algorithm is designed to operate on Landsat imagery only.

The ATCOR program is based on the assumption that it is possible to obtain a reasonable estimate for the reflectance of those portions of the earth's surface that correspond to the darkest pixels in a given Landsat segment. The haze level can then be determined from the brightness of these pixels. The result of using this algorithm was a correction which was finally applied to the Landsat image.

Haze level determination and correction.

In the ATCOR program, Band 4 is used to determine the haze level because, according to the haze model, the effect of haze is greatest in this band. The set of "darkest pixels" was obtained by taking the pixel from each line of Landsat data that had the lowest value in Band 4. An average minimum value was obtained by averaging the grey level values of these pixels. This value corresponds to the actual haze level. The average value for all Band 4 data in the segment was also computed. Next, average minimum grey values were computed for three arbitrary values of haze level. They were determined by interpolation in precomputed tables using the values of mean background reflectance and solar zenith angle. Further interpolation was then used to determine the grey level corresponding to the true haze level (Potter 1977).

Average background reflectance correction.

Once the haze level was known, the background reflectance for each

band could be determined. The first step was to calculate the average values for all the data in the segment for Bands 5, 6, and 7. Then the reflectances were interpolated from the tables. These values were printed out and could then be used to make the desired corrections.

Correction of the data.

Since the solar zenith angle was specified as a known value, the coefficients were then completely determined and could be applied to the Landsat image to make the desired corrections. This was a simple linear transform applied uniformly to the segment on any system.

Test 5.

The Air Force Avionics Laboratory (AFAL) algorithm for image normalization (Crouch and Leonard 1979) was scheduled to be evaluated, but the test was never performed. The procedure, however, is very similar to that used in Test 1. Normalization is achieved by matching areas of known reflectance to density, and then redistributing densities to produce a normalized image. The major difference between the AFAL approach and the Test 1 approach is that, in the latter, coefficients of the density vs. reflectance equation are obtained directly while in the AFAL algorithm, regression is used with a group density-reflectance pairs. This test would have used the black and white imagery described for Test 1.

RESULTS

Three of the algorithms described in the previous section (Tests 1-3) were evaluated for their usefulness to the Defense Mapping Agency in MC&G production. Both subjective and metric evaluations were made to determine the usefulness of output imagery and the degree of normalization according to the definition given earlier.

Subjective Evaluation

The subjective evaluation was conducted in two phases: data acquisition, and data processing and analysis. Only the results of Test 1 were evaluated.

The data were acquired using twenty experienced image analysts with varying backgrounds, and the images were scored using ten scales of image quality and perturbation. A total of 68 images were evaluated.

The analysis and processing of data consisted of compiling, eliminating statistical outliers, reducing the data set by principal components analysis, comparing results for unaltered analog image pairs with those for corresponding normalized image pairs, and drawing statistical inferences from the results.

High correlation between the seven image quality or utility scales enabled those scores to be combined into a single composite score. There was also high correlation between the three perturbation scales which permitted them to be combined into a second composite score. These two composite scores were used for the remainder of the analysis.

To show the degree of normalization, a difference score was computed for each analog (non-normalized) pair and each normalized pair using the two composite scores; then corresponding difference scores were compared. The intention was to remove the effect of image degradation due to the digitization process. The difference between each analog image's score and its corresponding normalized score on each of the composite measures was also examined to determine the preservation of

additional information was determined
in order to determine the coefficient for a
normalization based on background
reflectance, solar zenith angle and image type.

~~image's score and its corresponding~~ normalized score on each of the composite measures was also examined to determine the preservation of quality.

The most important result of the subjective evaluation was that the normalization algorithm demonstrated a strong probability of success. This finding coincides with what can readily be observed in most of the imagery, that is the normalized images appear "similar". The results clearly show a significant loss of information content, but they also clearly indicate that this loss was due to the digitization of imagery rather than the normalization algorithm.

Metric Evaluation

The metric evaluation was intended to provide an objective measure of the success of various tested algorithms in normalizing imagery. This involved rating the similarity of the output image pairs as compared to the input image pairs, and evaluating the preservation of image quality. The evaluation of image quality, however, was determined to be best accomplished with the subjective procedures, and thus was not pursued in the metric evaluation.

Two types of objective evaluation were utilized: evaluation of image histograms and evaluation of the power spectra generated by the two dimensional discrete Fourier transform. The histogram evaluation for Tests 1 and 2 included mean and standard deviation comparisons before and after normalization to reveal changes in the histograms. For Test 3, where the statistics were compiled by the contractor (ERIM), only the means of the histograms were available. The power spectra were calculated for most of the imagery; but since inspection showed that no meaningful data were being obtained, the process was discontinued.

Several detailed comparisons of derived data vs. ground truth were also made. These comparisons were particularly important for the hydrographic color imagery of Test 2, where temporally separated pairs were not always available (Gerson et al 1981). Two types of ground truth data were used: digital photometer "spot" observations taken from the research vessel, and analog photometer data taken by divers swimming near the surface of the water between markers which were anchored to the bottom. Comparisons were made by matching appropriate pixels derived from the photography with ocean bottom areas being measured by these two methods.

The data derived from Test 3 were analyzed by extracting histograms of all Landsat MSS bands before and after normalization. Ratios were then taken between these means in order to reveal changes that may have occurred in the normalization process.

Analysis of results.

The tests discussed above produced numerous output images and dozens of tables which were used to support the conclusions of this experiment. The results of the tests indicated some of the problems involved in defining evaluation procedures for imagery, as well as the difficulties in normalizing images. In general it can be said that the normalization techniques tested gave good results for black and white terrestrial imagery, and poorer results for color hydrographic imagery and Landsat.

Ideally, the approach used in Tests 1 & 2 should work very well since reflectance is a property of the object being imaged. The technique will normalize to a "standard" image, a highly desirable result, and information content should not be affected since transformations will be applied uniformly to each pixel. In reality, however, several problems exist. There is a contrast stretch, that occurs in this procedure which could affect human observers. This produced a

negative effect in the hydrographic imagery because it increased visible specular reflectance. The effects of digitization also proved to be disruptive in the subjective evaluation. Complicating factors reduced the effectiveness of this approach in both tests, but much more so in Test 2 on hydrographic color imagery.

Landsat imagery was not evaluated in the subjective evaluation. In the metric evaluation the Tassled Cap algorithm showed close comparisons in Bands 4 and 5, but poor results in Bands 6 and 7 when evaluated by individual band histogram comparisons. This can be explained by the actual changes in vegetation characteristics which took place between image acquisitions, and the sensitivity of these bands to those changes.

CONCLUSIONS

The following conclusions and recommendations were developed during the course of experimentation and evaluation of results.

Specific Conclusions from Tests

1. The reflectance calibration method of Test 1 can normalize terrestrial black and white imagery for specified image content if extreme care is taken in selecting and evaluating the area of known reflectance, and in selecting the area of minimal reflectance.

2. The reflectance calibration method of Test 2 fails to account for many of the complexities involved in the processing of color photography, the remote sensing of energy through the air-water column, and the determination and measurement of actual (vs. apparent) reflectances of underwater materials. The method may, however, have the potential for producing good results if a way can be found to accurately identify an area of known reflectance underwater. It may also be more suitable if used for normalizing to actual bottom reflectances rather than to those observed from the water's surface. In this way, water column variations could be accounted for in the normalization procedure, and the method could be used for change detection (which does not require the use of color film).

3. The Tassled Cap algorithm has the potential for normalizing Landsat scenes; but due to the inconclusive results in Test 3, this cannot be proven. The algorithm was designed for use in agricultural scenes, and needs readjustment to be utilized for cultural features. The results for Bands 4 and 5, which are most important for the interpretation of cultural features, were good; and thus the potential of this method seems to be very promising.

General Conclusions

1. Temporal Normalization is affected by:

a. Scene content. The difficulties in normalizing a scene often depend on the objects being imaged; for example, there are differences in bidirectional reflectance which are not accounted for in any of the tested algorithms. Dark objects on bright backgrounds (or vice versa) affect local ambient reflectance, which changes the apparent reflectance of the object. In addition, for some algorithms, it is necessary to know characteristics of objects within the scene. These are not always known, particularly in hydrographic imagery.

b. Imaging process. The path that light follows from its source to the recording media is complex. The largest variation in this experiment was between terrestrial and hydrographic imagery; the introduction of a water layer in the imaging process greatly increased the difficulties in normalizing imagery. In addition, the type of

recording media (black and white film, color film, solid state sensors) and the specific characteristics of each affect the normalization process.

c. Perturbation process. There are different perturbations that create a need for normalizing imagery. Uniform light haze is most easily normalized. Effects of sun angle (both elevation and azimuth) can be accounted for if severe bidirectional reflectance, as found in tree crowns and rows of crops, is not present. In hydrographic imagery, variations in sun angle can result in specular reflectance which cannot be removed. The introduction of a water column also adds turbidity and interface effects which perturb the image.

2. The temporal normalization methods that have been evaluated each constitute only the beginnings of an approach to a specific temporal normalization task for a specific type of imagery. These methods need further development, and other types of methods (e.g. atmospheric models) need to be evaluated.

REFERENCES

Brooke, R.K. Jr. 1974, Spectral/Spatial Resolution Targets for Aerial Imagery, ETL-TR-74-3, Engineer Topographic Laboratories, Fort Belvoir, VA.

Crouch, L.W. and J.D. Leonard, Jr. 1979, Contrast Restoration of Aerial Imagery, Report Number RWF-771279, Air Force Avionics Laboratory, Wright Patterson AFB, OH.

Curran, T.R. and J.W. Ingram, Jr. 1974, Terrain Data of Mount Hayes D-4 Quadrangle, Fort Greely, Alaska, ETL-TR-74-7, Engineer Topographic Laboratories, Fort Belvoir, VA.

Dave, J.V. 1978, Extensive Datasets of the Diffuse Radiation in Realistic Atmospheric Models With Aerosols and Common Absorbing Gasses, Solar Energy, Volume 21, pp. 361-369.

Davis G. and C. Wilson 1981, Temporal Normalization of Landsat Data, Final Report, Environmental Research Institute of Michigan, Report Number 154000-11-F, Ann Arbor, MI.

Gerson, D.J., L.K. Fehrenbach, K.R. Piech, and D.W. Gaucher 1981, Derivation of Shallow Ocean Bottom Reflectance Values From Color Aerial Photography, Proceedings of the 1981 Symposium on Machine Processing of Remotely Sensed Data, pp. 269-275, West Lafayette, IN.

Kauth, R.J., P.F. Lambeck, W. Richardson, G.S. Thomas, and A.P. Pentland 1979, Feature Extraction Applied to Agricultural Crops As Seen By Landsat, LACIE Symposium, October 1978, Johnson Space Center, NASA, pp. 705-721, Houston, Texas.

Lillesand, T.M. and R.W. Kiefer 1979, Remote Sensing and Image Interpretation, John Wiley & Sons, New York, NY.

Lyzenga, D.R. and F.C. Polcyn 1979, Techniques for the Extraction of Water Depth Information From Landsat Digital Data, Report No. 129900-1-F, Environmental Research Institute of Michigan, Ann Arbor, MI.

Piech, K.R. and J.E. Walker 1974, Interpretation of Soils, Photogrammetric Engineering, Vol. 40, pp. 87-94.

Piech, K.R., D.W. Gaucher, N. Schimminger, and C. Rogers 1978, Photometric Calibration of Black and White Imagery, RADC-TR-78-53, Rome Air Development Center, Griffiss Air Force Base, NY.

Piech, K.R. 1980, Material Identification Using Broad Band Visible Data, Proceedings of the Society of Photo-Optical Instrumentation Engineers, Volume 238, August 1980, San Diego, CA.

Potter, J.F. 1977, The Correction of Landsat Data for the Effects of Haze, Sun Angle, and Background Reflectance, Proceedings of the 1977 Symposium on Machine Processing of Remotely Sensed Data, pp. 24-52, West Lafayette, IN.

Schimminger, E.W. 1980, Black and White Calibration for Signature Extension, Technical Report RADC-TR-80-286, Rome Air Development Center, Griffiss Air Force Base, NY.

Turner, R.E. 1981, Multiple Scattering Atmospheric Radiation Models, Proceedings of the Society of Photo-Optical Instrumentation Engineers, Volume 277, Washington, DC.

2-8

DT